Magnetic field dependence of quantized and localized spin wave modes in thin rectangular magnetic dots

2004 J. Phys.: Condens. Matter 16 7709

(http://iopscience.iop.org/0953-8984/16/43/011)

INSTITUTE OF PHYSICS PUBLISHING JOURNAL OF PHYSICS: CONDENSED MATTER

J. Phys.: Condens. Matter **16** (2004) 7709–7721 PII: S0953-8984(04)84341-8

Magnetic field dependence of quantized and localized spin wave modes in thin rectangular magnetic dots

G Gubbiotti[1,7], M Conti[2], G Carlotti[2], P Candeloro[3], E Di Fabrizio[3], K Yu Guslienko[4], A Andre[5], C Bayer[5] and A N Slavin[6]

[1] Istituto Nazionale Fisica della Materia, Unità di Perugia, Via Pascoli, 06123 Perugia, Italy
[2] Unità INFM and Dipartimento di Fisica, Università di Perugia, Via Pascoli, 06123 Perugia, Italy
[3] LILIT Beamline, TASC-INFM at Elettra, SS14 km163.5, 34012 Basovizza, Trieste, Italy
[4] Materials Science Division, Argonne National Laboratory, 9700 South Cass Avenue, Argonne, IL 60439, USA
[5] Fachbereich Physik und Forschungsschwerpunkt MINAS, Technische Universität Kaiserslautern, 67663 Kaiserslautern, Germany
[6] Department of Physics, Oakland University, Rochester, MI 48309, USA

E-mail: gubbiotti@fisica.unipg.it

Received 28 July 2004, in final form 22 September 2004
Published 15 October 2004
Online at stacks.iop.org/JPhysCM/16/7709
doi:10.1088/0953-8984/16/43/011

Abstract

The magnetic field dependences of the frequencies of standing spin-wave modes in a tangentially magnetized array of thin rectangular permalloy dots (800 × 550 nm) were measured experimentally by a Brillouin light scattering technique and calculated theoretically using an approximate size-dependent quantization of the spin-wavevector components in the dipole-exchange dispersion equation for spin waves propagating in a continuous magnetic film. It was found that the inhomogeneous internal bias magnetic field of the dot has a strong influence on the profiles of the lowest spin-wave standing modes. In addition, the dynamic magnetization distributions found for both longitudinally and transversely magnetized long magnetic stripes gives a good approximation for mode distributions in a rectangular dot magnetized along one of its in-plane sides. An approximate analytic theory of exchange-dominated spin-wave modes, strongly localized along the dot edge that is perpendicular to the bias magnetic field, is developed. A good quantitative agreement with the results of the BLS experiment is found.

(Some figures in this article are in colour only in the electronic version)

1. Introduction

It has been shown by Brillouin light scattering (BLS) spectroscopy [1] that the lowest spin-wave mode in the spectrum of a transversely magnetized micrometre-width thin permalloy

[7] Author to whom any correspondence should be addressed.

stripe with rectangular cross-section (and in the spectrum of a tangentially magnetized thin rectangular dot) is localized in regions of strong inhomogeneity of the internal magnetic field near the stripe edges. A similar edge localized mode was observed in in-plane magnetized cylindrical dots by Gubbiotti *et al* [2]. It has been also shown in [1] that this localized mode, being the lowest in frequency in the spectrum, is nevertheless dominated by exchange interaction. These ideas about the nature of the lowest mode in the stripe spectrum were confirmed by direct measurements using the spatially resolved Kerr technique carried out by the group of Crowell [3]. Further numerical calculations conducted in [4, 5] have demonstrated possible spatial profiles of such localized modes (see e.g. figure 5 in [4] and figure 6 in [5]) while further experimental investigations by Bayer *et al* [6] have shown that several localized exchange-dominated modes can be formed near the edge of a transversely magnetized long magnetic stripe if the external magnetic field is sufficiently large.

In the current paper we present experimental data on the magnetic field dependence of the frequencies of quantized and localized spin-wave modes in the spectrum of a submicron-sized rectangular magnetic dot, and demonstrate that the lowest mode in this spectrum can be identified as a mode having exchange-dominated localization along the direction of the bias magnetic field. We also develop a simple approximate analytic theory based on the theory of Mathieu functions, which describes the spatial profiles of such localized modes and allows us to calculate the frequencies of these modes as functions of the external magnetic bias field.

Recently, several authors have investigated both experimentally and numerically the spin-wave modes existing in the regions in a magnetic element where the static magnetization varies with coordinate (edge domains or unsaturated parts of the sample) [7–9]. It should be stressed that in the current paper we are considering spin-wave modes localized near the edge of the magnetic element, but still in the *fully saturated region* where static magnetization is almost constant and parallel to the external bias magnetic field. In other words, we are working in the case of strong external magnetic fields in terms of [7–9]. The paper is organized as follows. In section 2 we describe the BLS measurements of the rectangular permalloy dots while in section 3 analytical and numerical calculations of the localized spin-wave modes in thin rectangular elements are presented. The comparison of the experimental data and developed theory is done in section 4. Finally, the conclusions are drawn in section 5.

2. Experiment

A magnetic array of rectangular permalloy ($Ni_{81}Fe_{19}$) dots was fabricated at the Elettra synchrotron radiation facility, LILIT beamline [10], exploiting x-ray lithography in combination with a lift-off process [11]. The x-ray mask (necessary to perform the lithography) was a silicon nitride (Si_3N_4) membrane, 100 nm thick, coated with a base plating of Cr–Au. Electron beam lithography was used to fabricate the Au absorbing structures of the mask. A permalloy ($Ni_{81}Fe_{19}$) layer with nominal thickness of $L = 30$ nm was evaporated over the resist pattern; during the evaporation the pressure was in the range $(3.5–5) \times 10^{-6}$ Torr. The rectangular dots have lateral dimensions $l = 800$ nm and $w = 550$ nm and separation $\Delta = 200$ nm. Based on our previous experience with permalloy dots of different shapes, the above value of the interdot distance Δ is large enough to guarantee negligible inter-dot magnetostatic interaction. During the fabrication process, part of the permalloy film was left unpatterned in order to compare the experimental results of the patterned region and of the unpatterned one. A detailed magnetic characterization of such an array of dots accomplished by magnetic force microscopy, magneto-optical Kerr effect and micro-magnetic simulations is presented elsewhere [12, 13].

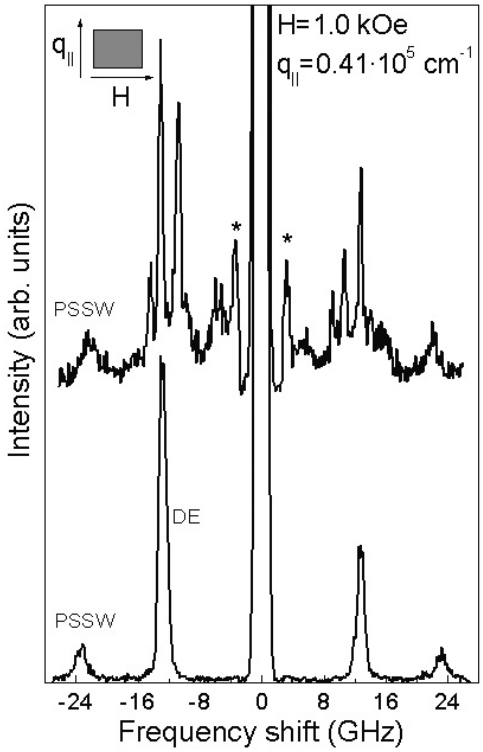

Figure 1. The BLS spectra measured at the light incidence angle $\theta = 10°$ and 1.0 kOe external field, for the patterned (upper panel) and the continuous reference film (lower panel). The two peaks close to the central elastic peak (indicated by asterisks in the upper panel) are artefacts produced by the mechanical shutter placed at the entrance of the interferometer to maintain the alignment of the Fabry–Perot cavity.

The BLS measurements were carried out at room temperature at the GHOST laboratory of the University of Perugia [14]. Light from a single mode diode-pumped solid state laser ($\lambda = 532$ nm), typically with a power of 200 mW and polarized in the incidence plane, was focused onto the sample surface, using a camera objective of numerical aperture 2 and focal length 50 mm. The back-scattered light, polarized perpendicular to the scattering plane, was collected by the same objective used for the focalization and analysed in a high-contrast, tandem (3 + 3) passes Sandercock-type tandem Fabry–Perot interferometer [15]. A bias external magnetic field, variable between 0 and 3 kOe, was applied parallel to the film surface and perpendicular to the plane of incidence of light. In the backscattering geometry, the conservation of momentum in the photon–magnon interaction implies that the transferred spin-wave wavevector parallel to the film surface is linked to the optical wavevector k_i and to the angle of incidence θ_i by the equation $q_\parallel = 2k_i \sin\theta_i$.

In figure 1 a typical BLS spectrum of the arrays of rectangular dots (upper part) is compared to that of the continuous unpatterned film (lower part); the incidence angle was $\theta = 10°$, corresponding to a wavenumber $q_\parallel = 0.41 \times 10^5$ cm^{-1}. In the spectrum of the continuous film two peaks are visible, the DE peak at 12.9 GHz and the first perpendicular standing spin-wave (PSSW) at 23.5 GHz, whereas the BLS spectrum of the patterned film reveals at least four peaks in the frequency range between 12 and 17 GHz, besides the bulk one at 23.5 GHz. A best fitting procedure of both the DE and the bulk modes in the unpatterned film as a function of the

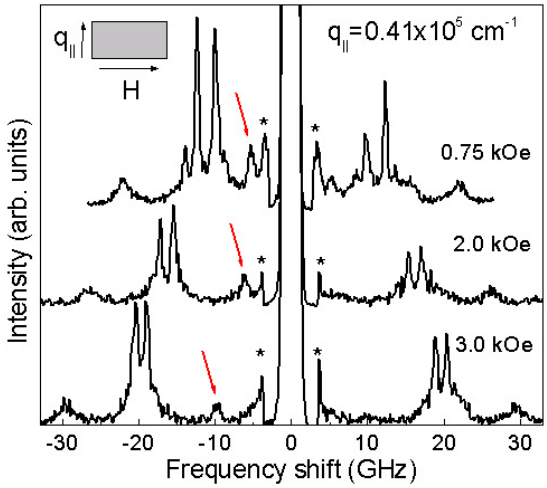

Figure 2. Magnetic field dependence of the BLS spectra of the rectangular permalloy element for the fixed incidence angle of light $\theta = 10°$.

incidence angle of light provides a film thickness of 27 nm, in good agreement with the nominal thickness of 30 nm, and the values found for the other parameters, the saturation magnetization $4\pi M_s = 10.2$ kOe, and the non-uniform exchange constant $\alpha = 2.5 \times 10^{-13}$ cm^2. All these modes observed for the patterned permalloy sample are dispersionless and are observed in a large wavevector range, as reported in our previous paper [16].

In figure 2, a series of BLS spectra for the patterned sample measured at different values of the magnetic field applied and $q_\parallel = 0.41 \times 10^5$ cm^{-1} are shown. The directions of the applied field and the in-plane transferred wavevector are shown in the figure insets by the arrows. The presence of a low frequency mode (indicated by the arrows) is clearly visible in the spectra measured at large fields because it is at larger distance from the elastic peak. The field dependence of the frequency of this mode will be calculated in the next section.

3. Theory of localized spin-wave modes

For the theoretical interpretation of the above described BLS experiment we shall use the approximate theory of the spin-wave spectrum in a tangentially magnetized thin rectangular magnetic elements (shown in figure 3) formulated in our recent paper [17]. We use the Cartesian coordinate system with the Oz axis directed perpendicular to the plane of the rectangular element.

We assume that the spins at the surfaces of the rectangular element that are perpendicular to the axis Oz are unpinned (i.e. there is no surface anisotropy). In that case the lowest spin-wave modes in this element have a uniform distribution of the variable magnetization along the element thickness L, i.e. we consider the modes with the wavevector component $k_z = 0$. Denote the element width as w, length l, and assume that $l \geqslant w$. Our theory is based on the approximate diagonal dispersion equation for dipole-exchange spin waves in a continuous magnetic film (see equation (7) in [17]) and the assumption that to calculate mode frequencies in a thin ($L \ll w$, $L \ll l$) magnetic element we can simply use the discrete values of the in-plane spin-wavevector $\kappa_{mn}^2 = k_{mx}^2 + k_{ny}^2$ quantized due to the finite in-plane sizes of the rectangular magnetic element (m, n are the integer indices to distinguish different spin-wave modes).

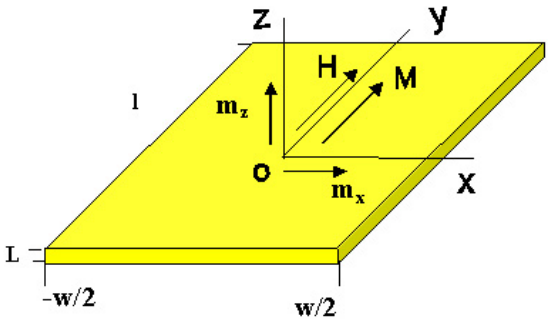

Figure 3. Thin rectangular magnetic element and the system of the coordinates.

The quantization conditions, determining the discrete values of the wavevector projections along the in-plane axes x and y, are given by equations (3) and (5) in [17]. Since the internal bias magnetic field inside the rectangular element (figure 3) is inhomogeneous, it is necessary to know the planar spatial distribution of variable magnetization in each particular spin-wave mode of the element to be able to calculate the effective internal bias field for this mode using equations (8), (9) in [17]. We also assume that the two-dimensional in-plane distribution of the variable magnetization $m_{mn}(x, y)$ in any spin-wave mode of a rectangular element can be represented as a product of the eigenfunctions of longitudinally $\Lambda_m(k_m x)$ and transversely $T_n(k_n y)$ magnetized infinitely long magnetic stripes:

$$m_{mn}(x, y) = M_s \Lambda_m(k_{mx} x)\, T_n(k_{ny} y). \tag{1}$$

It is worth noting that, although the transverse (along the element's thickness) variable z is not explicitly present in equation (1), the finite thickness L of the rectangular magnetic element is taken into account in our calculations.

In particular, the profiles of functions $\Lambda_m(k_{mx} x)$ characterizing the spin-wave eigenmodes in a longitudinally magnetized magnetic stripe (having thickness L, width w and $L \ll w$) are strongly dependent on the stripe's aspect ratio, L/w. The eigenfunctions $\Lambda_m(k_{mx} x)$ are defined by equation (10) in [18]. These eigenfunctions are of a purely dipolar nature and have the usual cosinusoidal profile with relatively strong 'pinning' at the edges for low-frequency modes due to the inhomogeneity of the dynamic dipolar field near the lateral edges of the stripe. This pinning strongly depends on the stripe's aspect ratio, L/w. The characteristic values of the in-plane mode wave number k_{mx} are approximately determined from equation (11) in [18].

The situation with the eigenfunctions $T_n(k_{ny} y)$ characterizing the spin-wave eigenmodes in a transversely magnetized magnetic stripe (having thickness L, width l and $L \ll l$) is much more complicated due to the strong inhomogeneity of the static internal magnetic field inside the transversely magnetized magnetic stripe along its width. This inhomogeneity is also strongly dependent on the stripe's aspect ratio L/l and, therefore, is different for different element thicknesses. Below we shall try to find spatial profiles of the eigenfunctions $T_n(k_{ny} y)$ in that case both numerically and analytically.

The coordinate-dependent internal static magnetic field can be easily calculated using the effective coordinate-dependent demagnetizing factor $N_{yy}(y)$ [19, 20] (see e.g. a particular case of equation (16) in [19]). Therefore, the non-uniform internal bias magnetic field inside a transversely magnetized magnetic stripe can be expressed in terms of the uniform external bias field H and saturation magnetization M_s as

$$H_i(y) = H - 4\pi M_s N_{yy}(y). \tag{2}$$

It should be noticed that equation (2) has physical meaning only in the spatial region where $H_i(y) \geqslant 0$. It was shown in [21] that in the narrow regions near the lateral edges of the stripe (edge domains) where static magnetization is not parallel to the bias field the equation (2) gives negative values for H_i and it should be assumed that in these regions $H_i = 0$. Below we shall only consider the regions in the magnetic elements that are completely saturated by the external bias field.

In the case of a transversely magnetized long magnetic stripe the usual system of the linearized Landau–Lifshitz equation of motion and Maxwell equations in the magnetostatic limit can be reduced to the following integro-differential equation for the variable magnetization $\boldsymbol{m}(y)$:

$$\left[-\alpha\omega_M \frac{d^2}{dy^2} + \omega_{H_i}(y)\right]\hat{I}\boldsymbol{m}(y) = -i\omega\hat{T}\boldsymbol{m}(y) - \frac{\omega_M}{4\pi}\int_{-l/2}^{l/2} dy'\,\hat{G}(y, y')\boldsymbol{m}(y'), \tag{3}$$

where

$$\boldsymbol{m}(y) = \begin{pmatrix} m_x(y) \\ m_z(y) \end{pmatrix}, \qquad \hat{I} = \begin{pmatrix} 1 & 0 \\ 0 & 1 \end{pmatrix}, \qquad \hat{T} = \begin{pmatrix} 0 & -1 \\ 1 & 0 \end{pmatrix}, \tag{4}$$

$$\hat{G}(y, y')_= \begin{pmatrix} 0 & 0 \\ 0 & G_{zz}(y, y') \end{pmatrix}, \qquad G_{zz}(y, y') = \frac{2}{L}\ln\left[\frac{(y - y')^2}{(y - y')^2 + L^2}\right], \tag{5}$$

$\omega_{H_i}(y) = \gamma H_i(y)$, $\omega_M = 4\pi\gamma M_s$, γ is the gyromagnetic ratio, α is the exchange stiffness measured in cm^2, ω is the spin-wave mode frequency, and $\hat{G}(y, y')$ is the tensor of magnetostatic kernels for long magnetic stripe ($w \to \infty$) averaged over the thickness coordinate z [22].

It is reasonable to assume that in the case of a thin transversely magnetized stripe the boundary conditions for the variable magnetization at the lateral edges of the stripe will be similar to the effective 'dipolar pinning' conditions obtained in the case of a longitudinally magnetized stripe (see equation (8) in [18]).

Numerical solution of equation (3) in the case when dynamic dipole–dipole interaction (described by the integral term in equation (3)) is dominant and the exchange interaction (described by the differential term in (3)) is negligible yields the magnetization distributions that, although not exactly cosinusoidal due to the inhomogeneity of the bias magnetic field, are nevertheless sufficiently similar to the dipolar eigenfunctions of the longitudinally magnetized stripe (defined by equation (10) in [18]). We can use these functions in our approximate calculations assuming that in the dipolar region $T(k_{ny}y) \cong \Lambda_n(k_{ny}y)$, and the characteristic values of the in-plane mode wavenumber k_{ny} are approximately determined from equation (11) in [18] where the element's width w is replaced by the element's length l. We note that this assumption will be correct only for sufficiently large magnetic elements having width greater than roughly 1 μm. In a smaller element the effect of dipolar localization of the lowest dipolar spin-wave mode near the centre of the element (see [17]) does not take place.

In the case when the spin-wave mode is localized somewhere and the exchange interaction is dominant, the spatial distributions of the spin-wave modes are quite different from the dipolar case. It is known [1, 3] that in this case spin-wave modes can be presented as localized near the stripe edges. Let us try to find the exchange-dominated spin wave eigenfunctions $T_\eta(k_{\eta y}y)$ of a transversely magnetized stripe both numerically and analytically. We changed notation for the quantization index $n \to \eta$ of these eigenfunctions to distinguish the exchange-dominated eigenfunctions $T_\eta(k_{\eta y}y)$ from the dipole-dominated eigenfunctions $\Lambda_n(k_{ny}y)$.

If the exchange interaction is dominant, we can neglect in zero approximation the integral in equation (3) and can formulate the following eigenvalue problem to find the eigenvalues λ_η and the eigenfunctions $T_\eta(k_{\eta y}y)$ of variable magnetization in a transversely magnetized

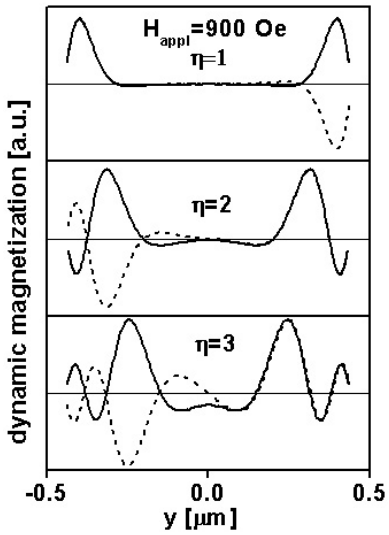

Figure 4. The dynamic magnetization mode profiles for a transversely magnetized stripe ($L = 33$ nm, $w = 1000$ nm, $4\pi M_s = 10.2$ kOe, $\alpha = 2.5 \times 10^{-13}$ cm^2).

magnetic stripe:

$$\left[-\alpha\frac{\mathrm{d}^2}{\mathrm{d}y^2} + \frac{\omega_{H_i}(y)}{\omega_M}\right]T_\eta(y) = \lambda_\eta T_\eta(y). \tag{6}$$

We note that the variable internal bias magnetic field in this problem is defined by equation (2). That is, we included into consideration in equation (6) the static dipolar field but neglected its dynamical part. This part will be accounted for in the form of diagonal matrix elements on the exchange-dominated eigenfunctions of the differential operator in equation (6).

The analytic solution of equation (6) is difficult to find due to the rather complicated coordinate dependence of the internal field $H_i(y)$ (2), but numerical solutions can be easily found. These solutions found for the case of a thin permalloy stripe ($L = 33$ nm, $w = 1000$ nm, $4\pi M_s = 10.2$ kOe, $\alpha = 2.5\times10^{-13}$ cm^2) transversely magnetized by the uniform external bias magnetic field 900 Oe are shown in figure 4. It turns out that two eigenfunctions (symmetric and anti-symmetric) correspond to each eigenvalue λ_η of the spectral problem (6), i.e. the corresponding spin-wave frequencies are degenerated. The eigenfunctions with the lowest indices $\eta = 0, 1, 2, 3$ are strongly localized near the stripe edges. With the increase of the mode index, localization diminishes and more nodes appear in the mode profile. We note that a similar frequency degeneracy of the symmetric and anti-symmetric edge modes was also found in the numerical micromagnetic simulations of the normal modes of a nano-sized rectangular prism by Grimsditch *et al* [5].

Let us now try to find approximate expressions for the exchange-dominated spin-wave eigenfunctions $T_\eta(k_\eta y)$ analytically. To achieve this goal, let us replace in equation (6) the real coordinate-dependent internal magnetic field $H_i(y)$ (2) by a model field $H_M(y)$

$$H_M(y) = \frac{H_{M0}}{2}\left[1 + \cos\left(\frac{2\pi}{l}y\right)\right] \tag{7}$$

which has a similar shape, but for which equation (6) has a known analytic solution. Indeed, if we replace in equation (3) $H_i(y)$ by $H_M(y)$, this equation can be reduced to a standard form

of a Mathieu differential equation (see e.g. [23, 24]):

$$\left[\frac{\mathrm{d}^2}{\mathrm{d}\xi^2} + a_\eta - 2q(H_{\mathrm{M0}})\cos(2\xi)\right] T_\eta(\xi) = 0. \tag{8}$$

where

$$\xi = \frac{\pi y}{l}, \qquad a_\eta = \frac{\lambda_\eta}{\alpha(\pi/l)^2} - 2q(H_{\mathrm{M0}}), \qquad q(H_0) = \left(\frac{\gamma H_{\mathrm{M0}}}{4\omega_{\mathrm{M}}}\right)\frac{1}{\alpha(\pi/l)^2}, \tag{9}$$

and $\eta = 1, 2\ldots$ is the order of a periodic Mathieu function.

It is known from the theory of Mathieu equations [24] that there exists an infinite set of characteristic values $a_\eta(q)$ which yields even periodic solutions of the equation (8) $T^s_\eta(\xi) = Ce_\eta(\xi)$ $(\eta = 0, 1, 2, \ldots)$ called *even Mathieu functions* of the order η and another infinite set of characteristic values $b_{\eta+1}(q)$ which yields odd periodic solutions of the equation (8) $T^a_\eta(\xi) = Se_{\eta+1}(\xi)$ $(\eta = 0, 1, 2, \ldots)$ called *odd Mathieu functions* of the order of $\eta + 1$. For the typical parameters of the permalloy stripe ($l = 1.0\ \mu$m, $4\pi M_{\mathrm{s}} = 10.2$ kOe, $\alpha = 2.5 \times 10^{-13}$ cm^2, $H_{\mathrm{i}}(0) = H_{\mathrm{M0}} = 1.0$ kOe) the parameter $q(H_{\mathrm{M0}})$ in the Mathieu equation (8) is $q(H_0) \approx 80 \gg 1$. For the case of $q \gg 1$, it is possible to obtain a simple asymptotic expression for the characteristic values of the Mathieu equation (8) in the form ([24], p 126):

$$a_\eta(q) = b_{\eta+1}(q) \cong -2q + 2(2\eta + 1)\sqrt{q} - \tfrac{1}{4}(2\eta^2 + 2\eta + 1), \tag{10}$$

which leads to a simple expression for the eigenvalues in our original equation (6) in the form

$$\lambda_\eta(H_{\mathrm{M0}}) = \left[2(2\eta + 1)\sqrt{q(H_{\mathrm{M0}})} - \frac{1}{4}(2\eta^2 + 2\eta + 1)\right]\alpha\left(\frac{\pi}{l}\right)^2, \tag{11}$$

where the index $\eta = 0, 1, 2, \ldots$.

It is also possible to obtain explicit asymptotic expressions for odd and even Mathieu functions in the limit $q \gg 1$ in terms of the elementary functions [24]:

$$\begin{aligned} Ce_\eta(\xi, q) &= \Psi_{1\eta}(\xi, q) + \Psi_{2\eta}(\xi, q), \\ Se_{\eta+1}(\xi, q) &= \Psi_{1\eta}(\xi, q) - \Psi_{2\eta}(\xi, q), \end{aligned} \tag{12}$$

where

$$\begin{aligned} \Psi_{1\eta}(\xi, q) &= \frac{2^{\eta+1/2}\exp(2\sqrt{q}\sin\xi)\left[\cos\left(\frac{\xi}{2} + \frac{\pi}{4}\right)\right]^{2\eta+1}}{(\cos\xi)^{\eta+1}}, \\ \Psi_{2\eta}(\xi, q) &= \frac{2^{\eta+1/2}\exp(-2\sqrt{q}\sin\xi)\left[\sin\left(\frac{\xi}{2} + \frac{\pi}{4}\right)\right]^{2\eta+1}}{(\cos\xi)^{\eta+1}}. \end{aligned} \tag{13}$$

The Mathieu functions (12) for $q = 100$ and $\eta = 1, 2$ are shown in figure 5. It is clear that these functions are qualitatively similar to the numerically calculated solutions $T_\eta(k_{\eta y} y)$ of equation (6) with real internal bias field defined by equation (2) that are shown in figure 4. Both sets of solutions for low values of the index η are localized near the stripe edges and in both sets each eigenvalue corresponds to two degenerate eigenfunctions: symmetric and anti-symmetric with respect to the stripe centre. It is, however, clear that we cannot expect quantitative agreement between the localized solutions of equation (6) for two different coordinate dependences of the internal field as in the spatial interval near the stripe edge ($0.35 < y/l < 0.45$), where the spin-wave eigenfunction with low index η has a maximum, the absolute values of two fields $H_{\mathrm{i}}(y)$ and $H_{\mathrm{M}}(y)$ are substantially different. To achieve a quantitative agreement between the two models we can require that the fields $H_{\mathrm{i}}(y)$ and $H_{\mathrm{M}}(y)$ are close to each other near the edge of the stripe where the localized mode has a maximum. Then, for each given value of the uniform external bias field H we can determine

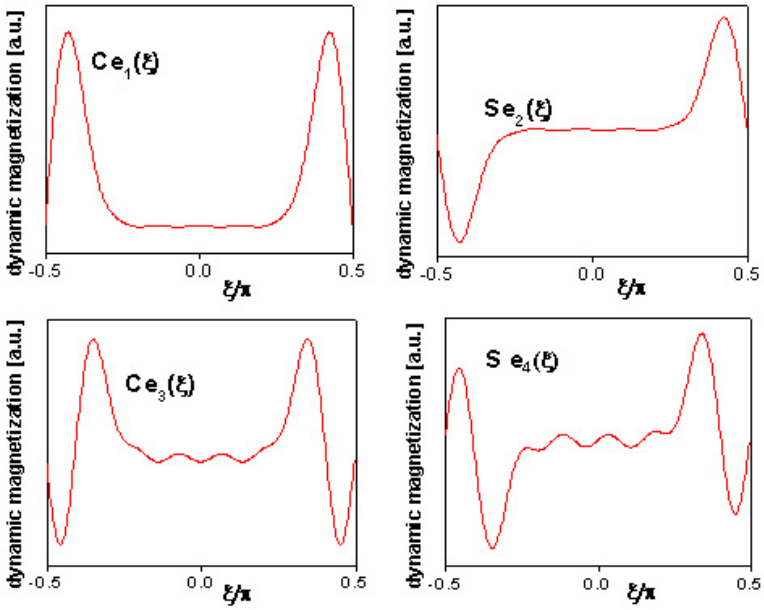

Figure 5. The even (left panel) and odd (right panel) Mathieu functions with low indices. $\xi = \pi y/l$ is the reduced coordinate along the stripe width.

the appropriate value of the parameter H_{M0} of the 'Mathieu model' field equation (7) from the minimization of the following functional:

$$J(H, H_{M0}) = \int_{y_1}^{y_2} [H_i(H, y) - H_M(H_{M0}, y)]^2 \, dy, \tag{14}$$

where the integration limits y_1, y_2 are chosen to include in the integration interval maximum of the corresponding Mathieu function of order η.

When the parameter H_{M0} of the Mathieu model field (7) is determined, we can find from equation (9) the parameter $q(H_{M0})$ which determines the profile of the Mathieu functions. The minimization procedure is illustrated in figure 6 for the Mathieu function of order $\eta = 1$ when the external bias magnetic field H is equal $H = 1.5$ kOe. The obtained value of the Mathieu parameter H_{M0} is $H_{M0} = 11.2$ kOe, which results for a typical permalloy stripe of the width $l = 1.0$ μm in a value of the q parameter (9) equal to $q(H_{M0}) = 10^3$.

To determine the characteristic values of the in-plane wavenumber $k_{\eta y}$ for the localized exchange-dominated spin-wave modes $T_\eta(k_{\eta y} y)$ existing in the strongly inhomogeneous internal bias field of the transversely magnetized stripe we shall use the analogy with usual exchange-dominated thickness spin-wave modes existing in the homogeneous internal bias field of in an infinite magnetic film (modes of the spin-wave resonance) [25]. Our eigenvalue problem equation (6) differs from the eigenvalue problem for the modes of spin-wave resonance (equation (11) in [20]) only due to the coordinate dependence of the internal bias field in our case. Thus, the structure of the expression for the eigenvalue should be similar in both problems, and we write the expression for our eigenvalue λ_η in the form analogous to the form of the eigenvalue expression in [25] (see equation (17) in [2]):

$$\lambda_\eta = \frac{\omega_H^\eta}{\omega_M} + \alpha k_{\eta y}^2, \tag{15}$$

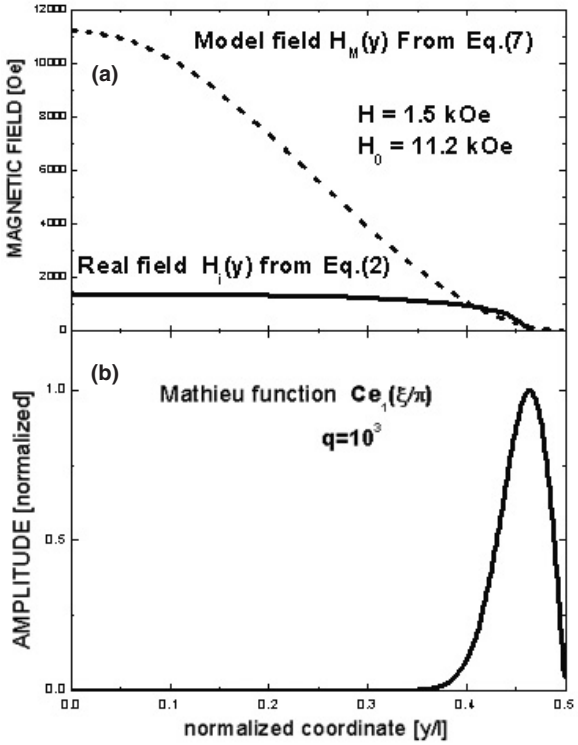

Figure 6. The model internal field profiles (a) and the first localized mode profile (b) in a transversely magnetized stripe.

where the frequency ω_H^η proportional to the effective internal magnetic field H_i^η ($\omega_H^\eta = \gamma H_\mathrm{i}^\eta$) for a spin wave mode is defined by the formula (obtained from equation (2))

$$\omega_H^\eta(H, H_{\mathrm{M0}}) = \gamma H - \omega_\mathrm{M} N_\eta(H_{\mathrm{M0}}). \tag{16}$$

The effective demagnetization factor N_η for the spin-wave mode with index η is defined by the expression

$$N_\eta(H_{\mathrm{M0}}) = \frac{\int \mathrm{d}y\, T_\eta^2(y, H_{\mathrm{M0}}) N_{yy}(y)}{\int \mathrm{d}y\, T_\eta^2(y, H_{\mathrm{M0}})}. \tag{17}$$

The integration in the integrals (17) is done along the whole region inside the stripe where the coordinate-dependent effective demagnetizing factor $N_{yy}(y)$ is positive.

Finally, using equations (11) and (15) we obtain an explicit approximate expression for the characteristic wavenumber k_η of the localized spin wave mode of order η:

$$k_{\eta y}(H, H_{\mathrm{M0}}) = \sqrt{\left[\lambda_\eta(H_{\mathrm{M0}}) - \frac{\omega_H^\eta(H, H_{\mathrm{M0}})}{\omega_\mathrm{M}}\right]\frac{1}{\alpha}}. \tag{18}$$

The frequency of the first exchange-dominated thickness mode of a rectangular dot ($m = 1$, $n = 1$, $p = 1$) was calculated using a standard formula [22]:

$$\omega_{mnp} = \omega_H^{mnp} + \alpha\omega_\mathrm{M}\kappa_{mnp}^2, \tag{19}$$

where the non-zero k_z-component of the wavevector is taken into account,

$$k_{mnp}^2 = k_{mx}^2 + k_{ny}^2 + k_z^2 = (m\pi/w)^2 + (n\pi/l)^2 + (p\pi/L)^2\,,$$

and the effective bias magnetic field for this mode ω_H^{mnp} was found using expressions similar to equations (8) and (9) in [14] for the following distribution of variable magnetization in the mode (1, 1, 1),

$$m_{m=1,n=1,p=1}(x, y, z) = M_s \cos\left(\frac{\pi x}{w}\right) \cos\left(\frac{\pi y}{l}\right) \cos\left[\frac{\pi}{L}\left(z + \frac{L}{2}\right)\right], \qquad (20)$$

that assumes unpinned surface spins at the top and bottom surfaces of the permalloy dot and total 'dipolar' pinning at the lateral edges.

Now we have all the necessary information to use the approximate formalism developed by Guslienko *et al* [17] (see equations (7)–(11) in [17]) for calculation of the magnetic field dependences of all the frequencies of the standing spin-wave modes observed in the tangentially magnetized sub-micron-sized rectangular permalloy dots in the above-described BLS experiments.

4. Comparison with experiment and discussion

We assume that the lowest mode in the experimentally measured spin-wave spectrum is the mode $m_{m=1,\eta=1}(x, y)$ which according to equations (1) and (6) has the form

$$m_{m=1,\eta=1}(x, y) = M_s \cos(k_{1x}x) Ce_1(\pi y/l), \qquad (21)$$

while the dipolar modes are described by sinusoidal functions given by equation (10) in [15] along both in-plane directions. The approximate profiles of the simplest spin-wave modes of a rectangular dot are shown in figure 7. The spin-wave eigenmode given by equation (21) is localized along the bias field direction near the rectangular element edges $y = \pm l/2$ (see figure 7(a)).

To calculate the dipolar modes of the rectangular magnetic element we used simple sinusoidal distributions of variable magnetization in the mode (see equation (10) in [14])

$$m_{mn}(x, y) = M_s \Lambda_m(k_{mx}x) \Lambda_n(k_{ny}y). \qquad (22)$$

We note that in contrast to the case of the dipolar localization described in [1], in our current experiment the longitudinal (along the bias field) size of the permalloy dot (0.8 μm) is so small that the dipolar localization of the lowest dipolar spin-wave modes does not take place and equation (21) including the first Mathieu function gives a reasonably good description of the first mode spatial distribution.

The results of comparison of our calculation with the results of the above BLS experiment for 800 × 550 nm permalloy rectangular elements are presented in figure 8. It is clear that our approximate theory gives a good quantitative description of the experiment in almost all the interval of the bias fields used. We notice that the slope of the exchange mode localized at the edge ($m = 1$, $\eta = 1$) is lower than that of the band of dipolar modes with the indices (m, n) and the mode profiles given by equation (22). This seems to be a characteristic feature of these spin-wave modes and has been already observed in tangentially magnetized cylindrical dots [2]. We can understand such a behaviour considering the fact that this mode is localized near the dot edges where the internal field is strongly inhomogeneous. With the increase of the applied bias field the profile of the internal bias field does not change qualitatively, and, therefore, the profile of the localized mode changes slowly with the variation of the applied field. This explains the relatively weak field dependence of the localized mode frequency on the applied magnetic field.

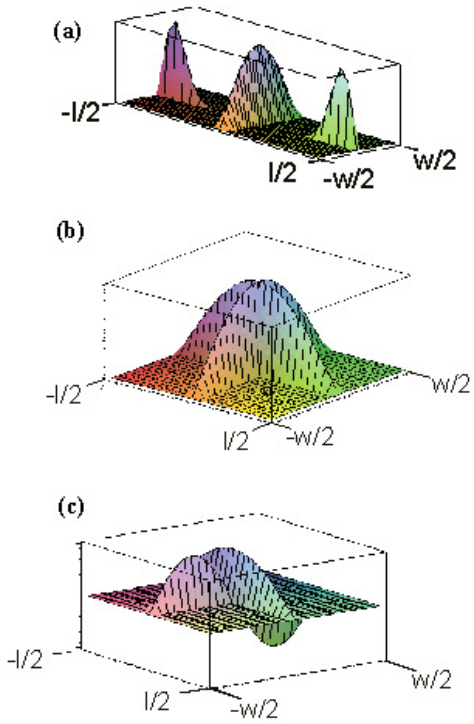

Figure 7. The spin-wave mode profiles in a rectangular dot magnetized along its side marked l: (a) the lowest exchange dominated localized mode with the indices $m = 1$, $\eta = 1$; (b) the first dipole dominated mode, $m = 1$, $n = 1$; (c) the dipole-dominated mode with the indices $m = 2$, $n = 1$.

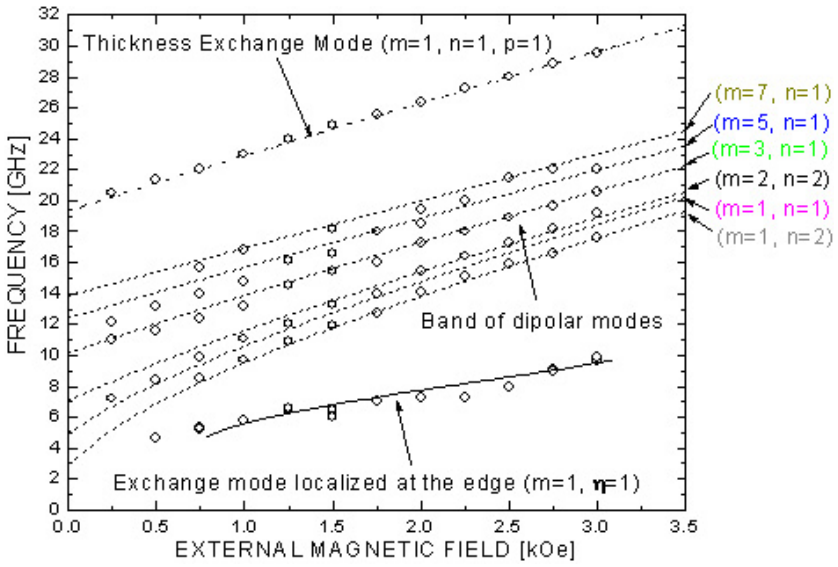

Figure 8. Comparison of experimental (open circles) and calculated (dotted line for thickness exchange mode, dashed lines for dipolar modes with the indices (m, n), solid line for exchange-dominated localized mode $m = 1$, $\eta = 1$) dependences of the spin-wave mode frequencies on the magnetic field intensity in the range 0.25–3.0 kOe. The frequency of the localized mode is calculated using equation (18) and the mode spatial distribution is given by equation (21).

5. Conclusions

Our calculations and experiments have demonstrated that the approximate qualitative theory based on the quantization of projections of the spin-wavevector in the dispersion equation for a continuous magnetic film gives a reasonably good quantitative description of the standing dipole-exchange spin-wave modes in nano-sized, non-interacting, thin rectangular magnetic dots. We were able to identify two types of spin-wave modes in a dot: the dipole-dominated (localized near the element centre) and the exchange-dominated (localized near the element edges), and to reproduce their frequency dependence on the intensity of the bias magnetic field.

Acknowledgments

This work was supported by the MURI grant W911NF-04-1-0247 from the Army Research Office of the USA, the Italian Ministry for the Instruction, University and Research (MIUR), the Deutsche Forschungsgemeinschaft (Grant No. Hi 380/15), and by the Oakland University Foundation. Work at ANL was supported by US Department of Energy, BES Materials Sciences under contract No. W-31-109-ENG-38. CB acknowledges support by the Studienstiftung des Deutschen Volkes.

References

[1] Jorzick J, Demokritov S O, Hillebrands B, Bailleul M, Fermon C, Guslienko K Y, Slavin A N, Berkov D V and Gorn N L 2002 *Phys. Rev. Lett.* **88** 3968
[2] Gubbiotti G, Carlotti G, Okuno T, Shinjo T, Nizzoli F and Zivieri R 2003 *Phys. Rev.* B **68** 184409
[3] Park J P, Eames P, Engebretson D M, Berezovsky J and Crowell P A 2002 *Phys. Rev. Lett.* **89** 277201
[4] Roussigne Y, Cherif S M and Moch P 2003 *J. Magn. Magn. Mater.* **263** 289
[5] Grimsditch M, Leaf G K, Kaper H G, Karpeev D A and Camley R E 2004 *Phys. Rev.* B **69** 174428
[6] Bayer C, Demokritov S O, Hillebrands B and Slavin A N 2003 *Appl. Phys. Lett.* **82** 607
[7] Bailleul M, Olligs D and Fermon C 2003 *Phys. Rev. Lett.* **91** 137204
[8] Bayer C, Park J P, Wang H, Yan M, Campbell C E and Crowell P A 2004 *Phys. Rev.* B **69** 134401
[9] Roussigne Y, Cherif S M and Moch P 2004 *J. Magn. Magn. Mater.* **268** 89
[10] http://www.elettra.trieste.it/experiments/beamlines/lilit
[11] Gerardino A, Di Fabrizio E, Nottola A, Cabrini S, Giannini G, Mastrogiacomo L, Gubbiotti G, Candeloro P and Carlotti G 2001 *Microelectron. Eng.* **57/58** 931
[12] Candeloro P, Kumar R, Di Fabrizio E, Conti M, Gubbiotti G, Carlotti G, Gerardino A, Zivieri R and Donzelli O 2003 *Japan. J. Appl. Phys.* **42** 3802
[13] Castrucci P, Scarselli M, Candeloro P, Di Fabrizio E, Conti M, Carlotti G, Gubbiotti G, Montocello F, Zivieri R and De Crescenzi M 2004 *Surf. Sci.* **566–568** 291
[14] http://ghost.fisica.unipg.it
[15] Sandercock J R 1982 *Light Scattering in Solids III* (*Springer Topics in Applied Physics* vol 51) ed M Cardona and G Güntherodt (Berlin: Springer) p 173
[16] Gubbiotti G, Candeloro P, Businaro L, Di Fabrizio E, Gerardino A, Zivieri R, Conti M and Carlotti G 2003 *J. Appl. Phys.* **93** 7595
[17] Guslienko K Yu, Chantrell R W and Slavin A N 2003 *Phys. Rev.* B **68** 024422
[18] Guslienko K Yu, Demokritov S O, Hillebrands B and Slavin A N 2002 *Phys. Rev.* B **66** 132402
[19] Joseph R I and Schlomann E 1965 *J. Appl. Phys.* **36** 1579
[20] Aharoni A 1998 *J. Appl. Phys.* **83** 3432
[21] Bryant P and Suhl H 1989 *Appl. Phys. Lett.* **54** 2224
[22] Guslienko K Yu and Slavin A N 2001 *Mater. Sci. Forum* **373–376** 217
[23] McLachlan N W 1964 *Theory and Application of Mathieu Functions* 1st edn (New York: Dover)
[24] Bateman H 1955 *Higher Transcendental Functions* vol 3 (New York: McGraw-Hill) p 126
[25] Kalinikos B A and Slavin A N 1986 *J. Phys. C: Solid State Phys.* **19** 7013